

## Random unitary matrices

This article has been downloaded from IOPscience. Please scroll down to see the full text article.

1994 J. Phys. A: Math. Gen. 27 4235

(<http://iopscience.iop.org/0305-4470/27/12/028>)

View [the table of contents for this issue](#), or go to the [journal homepage](#) for more

### Download details:

IP Address: 171.66.16.68

The article was downloaded on 01/06/2010 at 21:57

Please note that [terms and conditions apply](#).

## Random unitary matrices

Karol Życzkowski† and Marek Kuś†

† Instytut Fizyki, Uniwersytet Jagielloński, ul. Reymonta 4, 30-059 Kraków, Poland

‡ Centrum Fizyki Teoretycznej, Polska Akademia Nauk, al. Lotników 32/46, 02-668 Warszawa, Poland

Received 18 January 1994

**Abstract.** Methods of constructing random matrices typical of circular unitary and circular orthogonal ensembles are presented. We generate numerically random unitary matrices and show that the statistical properties of their spectra (level-spacing distribution, number variance) and eigenvectors (entropy, participation ratio, eigenvector statistics) confer to the predictions of the random-matrix theory, for both CUE and COE.

### 1. Introduction

Statistical ensembles of unitary matrices, introduced by Dyson [1] in order to describe spectral properties of quantum objects with many degrees of freedom like atomic nuclei, also proved to be useful descriptions in the case of relatively simple systems with few degrees of freedom exhibiting chaos in the classical limit [2, 3]. For autonomous (time-independent) systems a natural description is one in terms of a Hamiltonian (Hermitian) matrix and its eigenvalues (energies), whereas for systems periodically perturbed in time a more convenient characterization is provided by the unitary operator propagating the wavefunction of the system over one period of the perturbation. The relevant quantities are, in this case, connected with the properties of the eigenphases (phases of the eigenvalues) of the so-constructed propagator, i.e. quasi-energies of the system.

Numerous (mostly numerical) investigations [2, 3] have established, beyond doubt, close connections between chaos on the classical level and properties of the quantum energy (in the autonomous case) or quasi-energy spectra (in the time-periodic case). For systems which are fully chaotic, statistical properties of spectra, such as the distribution of spacings between adjacent levels  $P(s)$ , spectral rigidity  $\Delta_3(L)$  and number variance  $\Sigma^2(L)$  (at least for low values of  $L$ ) [4–7], are similar as in the appropriate ensembles of random matrices. The probability of finding two adjacent levels at a distance  $s$  goes to zero with decreasing  $s$ . The power of repulsion of levels, i.e. the rate of change of the probability density  $P(s)$  of the nearest-levels spacing  $s$  when  $s$  goes to zero depends on symmetries (mostly on the time-reversal invariance) of the system in consideration [3]. The highest degree of level repulsion,  $P(s) \sim s^4$ , characterizes the symplectic ensemble, to which typical time-reversal invariant chaotic systems with a half-integer spin pertain. In the unitary ensemble describing properties of typical time-reversal non-invariant chaotic systems one has  $P(s) \sim s^2$ , whereas for chaotic systems with time-reversal invariance and an integer spin the orthogonal ensemble with  $P(s) \sim s$  is appropriate. In contrast, the (quasi-)energy levels of generic classically regular systems are statistically uncorrelated, which leads to the Poissonian distribution of nearest-neighbour spacings [3] (level clustering). Also,

properties of scattering matrices for potentials in which the classical motion is chaotic are well described by the relevant ensembles of unitary random matrices [8–10].

It is relatively easy to generate random Hermitian matrices pertaining to different universality classes—the matrix elements of such matrices are statistically independent random variables drawn according to a Gaussian distribution with zero mean [5–7]. The only constraints are imposed by the algebraic conditions of symmetry (reality), hermiticity and symplecticity, involving pairs of elements. Hamiltonian of the time-periodic systems usually has the form

$$H = H_0 + \lambda H_1(t) \quad (1.1)$$

where  $H_1(t + T) = H_1(t)$ . In the simplest case of infinitely short ('kicking') perturbation when

$$H_1(t) = V_S \sum_{n=-\infty}^{\infty} \delta(t - nT) \quad (1.2)$$

where  $\delta$  is the Dirac delta function, the unitary one-step evolution operator is given as

$$U = U_0 U_1 = \exp(-iT H_0) \exp(-i\lambda V_S) \quad (1.3)$$

i.e. as a product of two unitary operators corresponding to the 'free' evolution and infinitely strong, instantaneous perturbation. In the following sections we recall the definitions of circular ensembles, and describe the methods of generating unitary and symmetric unitary matrices, also checking that matrices obtained really conform to the predictions of random matrix theory (RMT).

## 2. Random unitary and symmetric unitary matrices

Dyson's ensembles of matrices are defined as the subsets of the set of unitary matrices [1, 11]. Uniqueness of the ensembles is imposed by introducing measures invariant under appropriate groups of transformations. Specifically, the circular unitary ensemble (CUE) consists of all unitary matrices with the natural (normalized) Haar measure on the unitary group  $U_N$ . Let  $U$  be an arbitrary unitary matrix and let  $W$  and  $V$  be two such unitary matrices that  $U = WV$ . Then in a neighbourhood of  $U$

$$U + dU = W(1 + i dX)V \quad (2.1)$$

where  $dX$  is an infinitesimal Hermitian matrix with the elements  $dX_{ij} = dX_{ij}^1 + i dX_{ij}^2$ . The probability measure for CUE on the neighbourhood  $dU$  is thus

$$P_u(dU) = \mathcal{N}_u \prod_{i < j} dX_{ij}^1 \prod_{i < j} dX_{ij}^2 \quad (2.2)$$

where  $\mathcal{N}_u$  is a normalization constant. It is easy to check that a such-defined measure is invariant under arbitrary unitary transformations [1, 5] (and, in particular, independent of the choice of  $W$  and  $V$ ), hence proportional to the Haar measure.

In practical applications we usually investigate properties of individual matrices or at most of finite sets of them. From this point of view we found it convenient to define the notion of the CUE *sequence*. It is a sequence  $\{U_i\}$ ,  $i = 1, \dots, \infty$  of unitary matrices such that

$$\lim_{n \rightarrow \infty} \frac{1}{n} \sum_{i=1}^n f(U_i) = \int_{U_N} f(U) P_u(dU) \quad (2.3)$$

for functions  $f$  for which the right-hand side of the above equation exists. In many applications of the random matrix theory to the problems of quantum chaos one investigates an individual matrix representing the Hamiltonian or the propagator of the system and compares the results with the predictions of RMT. In order to formalize such a procedure we define a matrix  $U$  to be *typical of CUE with respect to the function  $f$*  if for an arbitrary CUE sequence  $\{U_i\}$  we have

$$f(U) = \lim_{n \rightarrow \infty} \frac{1}{n} \sum_{i=1}^n f(U_i). \tag{2.4}$$

Here we do not specify more precisely the nature and properties of the function  $f$ . In practical applications  $f$  can be e.g. the distribution of spacings between the nearest eigenphases or some correlation function of the spectrum, etc.

The circular orthogonal ensemble (COE) is defined on the set of all symmetric unitary matrices  $S = S^T = (S^\dagger)^{-1}$  by the property of being invariant under all transformations

$$S \rightarrow W^T S W \tag{2.5}$$

with arbitrary unitary  $W$  ( $T$  denotes the transposition). For every symmetric unitary matrix  $U$  we have

$$S = U^T U \tag{2.6}$$

with  $U$  some unitary matrix. In a neighbourhood of  $S$ ,

$$S + dS = U^T (1 + i dY) U \tag{2.7}$$

with  $dY$  real and symmetric, and the probability measure for COE is given as

$$P_o(dS) = \mathcal{N}_o \prod_{i < j} dY_{ij}. \tag{2.8}$$

Like in the case of CUE we introduce the notion of a COE *sequence*  $\{S_i\}$  by imposing the condition

$$\lim_{n \rightarrow \infty} \frac{1}{n} \sum_{i=1}^n f(S_i) = \int_{\text{COE}} f(S) P_o(dS) \tag{2.9}$$

and define a matrix  $S$  *typical of COE with respect to  $f$*  by demanding that

$$f(S) = \lim_{n \rightarrow \infty} \frac{1}{n} \sum_{i=1}^n f(S_i) \tag{2.10}$$

for an arbitrary COE sequence  $\{S_i\}$ .

### 3. Numerical generation of matrices typical of CUE

It is clear from the definitions given in the previous section that the elements of unitary matrices are not independent random variables, in contrast with the Hermitian case mentioned in the introduction. That is why numerical generation of such random matrices is more complicated. The apparently simplest way of generating random unitary matrices by exponentiating Hermitian ones taken from the Gaussian ensembles is unfortunately not acceptable. For example, the spectral properties of the matrix  $U = e^{iH}$  for  $H$  taken from the Gaussian ensemble of Hermitian matrices, due to multiple wrapping around the unit circle after exponentiation, are different from the properties of matrices from CUE. The solution consists, in fact, of finding a convenient parameterization of the space of unitary matrices by  $N^2$  independent parameters,  $N$  being the dimension of the matrices considered. Such a

parameterization is known at least from the times of Hurwitz [12] and uses the appropriate Euler angles. An arbitrary unitary transformation  $U$  can be composed from elementary unitary transformations in two-dimensional subspaces. The matrix of such an elementary unitary transformation will be denoted by  $E^{(i,j)}(\phi, \psi, \chi)$ . The only non-zero elements of  $E^{(i,j)}$  are

$$\begin{aligned} E_{kk}^{(i,j)} &= 1 & k = 1, \dots, N & \quad k \neq i, j \\ E_{ii}^{(i,j)} &= \cos \phi e^{i\psi} \\ E_{ij}^{(i,j)} &= \sin \phi e^{i\chi} \\ E_{ji}^{(i,j)} &= -\sin \phi e^{-i\chi} \\ E_{jj}^{(i,j)} &= \cos \phi e^{-i\psi} . \end{aligned} \quad (3.1)$$

From the above elementary unitary transformations one constructs the following  $N - 1$  composite rotations:

$$\begin{aligned} E_1 &= E^{(1,2)}(\phi_{12}, \psi_{12}, \chi_{12}) \\ E_2 &= E^{(2,3)}(\phi_{23}, \psi_{23}, 0) E^{(1,3)}(\phi_{13}, \psi_{13}, \chi_{13}) \\ E_3 &= E^{(3,4)}(\phi_{34}, \psi_{34}, 0) E^{(2,4)}(\phi_{24}, \psi_{24}, 0) E^{(1,4)}(\phi_{14}, \psi_{14}, \chi_{14}) \\ &\vdots \\ E_{N-1} &= E^{(N-1,N)}(\phi_{N-1,N}, \psi_{N-1,N}, 0) E^{(N-2,N)}(\phi_{N-2,N}, \psi_{N-2,N}, 0) \\ &\quad \dots E^{(1,N)}(\phi_{1N}, \psi_{1N}, \chi_{1N}) \end{aligned} \quad (3.2)$$

and finally forms the unitary transformation  $U$  as

$$U = e^{i\alpha} E_1 E_2 E_3 \dots E_{N-1} . \quad (3.3)$$

If the angles  $\alpha$ ,  $\phi_{rs}$ ,  $\psi_{rs}$ , and  $\chi_{1s}$  are taken from the intervals

$$0 \leq \phi_{rs} \leq \frac{\pi}{2} \quad 0 \leq \psi_{rs} < 2\pi \quad 0 \leq \chi_{1s} < 2\pi \quad 0 \leq \alpha < 2\pi \quad (3.4)$$

uniformly with respect to the Haar measure [12, 13]

$$P_U(dU) = \sqrt{N! 2^{N(N-1)}} d\alpha \prod_{1 \leq r < s \leq N} \frac{1}{2^r} d[(\sin \phi_{rs})^{2r}] d\psi_{rs} \prod_{1 < s \leq N} d\chi_{1s} . \quad (3.5)$$

we expect to obtain a matrix typical of CUE.

We have numerically generated  $N \times N$  unitary matrices by choosing the random angles  $\alpha$ ,  $\psi_{rs}$  and  $\chi_{1s}$  with an uniform distribution on the interval  $[0, 2\pi)$ . Additionally we have drawn random variables  $\xi$  with the uniform distribution on  $[0, 1)$  and we have taken the angles  $\phi_{rs}$  as  $\arcsin(\xi^{1/2^r})$  for  $r = 1, 2, \dots, N-1$ . A sequence of matrices generated in this way is a CUE sequence. Figure 1 presents the nearest-neighbour distribution  $P(s)$  obtained for 600 matrices of size  $N = 100$ . Note a fair coincidence with the approximate Wigner formula

$$P_U(s) = \frac{32}{\pi^2} s^2 \exp \left[ -\frac{4s^2}{\pi} \right] \quad (3.6)$$

represented by a full curve.

In order to study the long-range correlations of the spectrum we computed the average number of levels  $\langle N_S(L) \rangle$  in an interval of the length  $L$ , and the number variance  $\Sigma^2(L) = \langle N_S^2(L) \rangle - \langle N_S(L) \rangle^2$ . Numerical results obtained from the same ensemble of

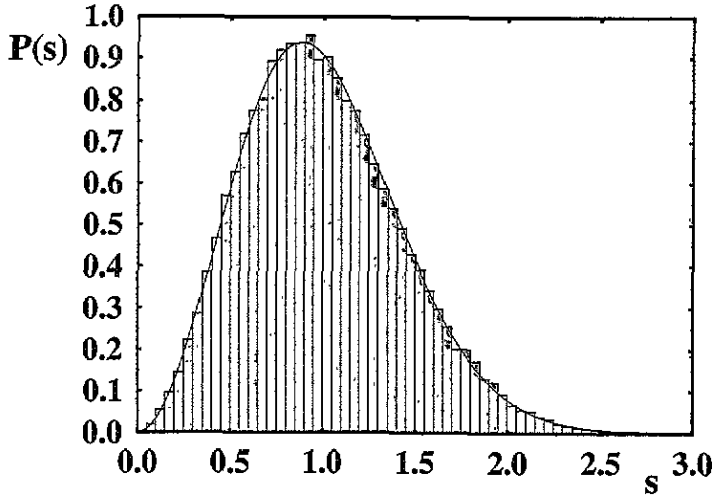


Figure 1. Nearest neighbour distribution for 600  $100 \times 100$  matrices typical to CUE.

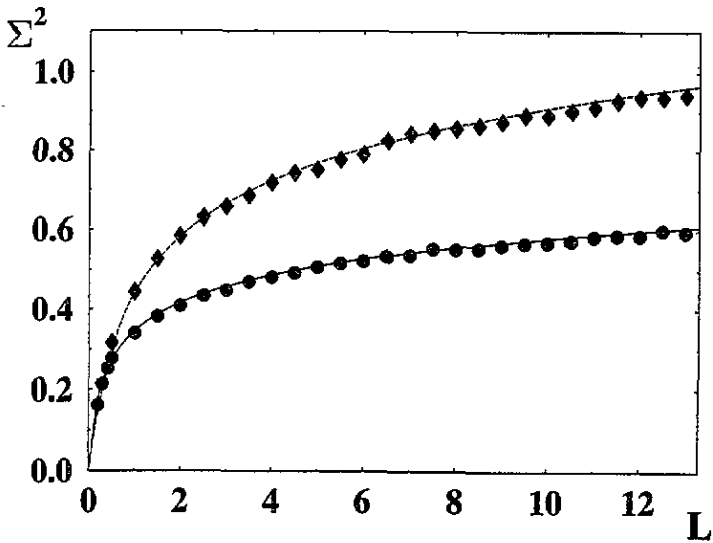


Figure 2. Number variance  $\Sigma^2(L)$  for CUE ( $\circ$ ) and COE ( $\diamond$ ). Full and dashed lines stand for the formulae (3.7) and (4.6).

600 matrices typical to CUE are represented by circles in figure 2. The full curve represents the CUE/GUE formula approximated (for  $L > 1$ ) by [7, 2]:

$$\Sigma_U^2(L) = \frac{1}{\pi^2} (\ln(2\pi L) + 1 + \gamma) \tag{3.7}$$

where  $\gamma \approx 0.577 \dots$  is the Euler constant. To save the computing time we have stopped the computation at the point where an agreement between the numerical results and the theoretical behaviour (3.7) is evident.

Diagonalizing the unitary random matrices we obtained not only their eigenvalues, but also eigenvectors  $|\varphi_l\rangle$ ,  $l = 1, \dots, N$ ; each represented in the initial basis by  $N$  complex

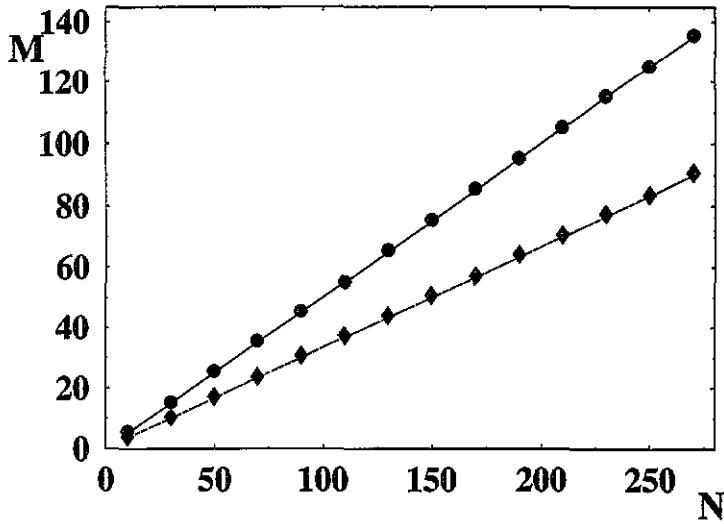


Figure 3. Number of relevant states  $M$  as a function of the matrix size  $N$  for CUE (o) and COE (◊).

coefficients  $c_{lk}$ . Localization properties of eigenvectors depend on their components  $y_{lk} = |c_{lk}|^2$ . The inverse participation ratio  $\mu_l$  of the  $l$ th eigenvector is defined as [14]

$$\mu_l = N \sum_{k=1}^N y_{lk}^2. \tag{3.8}$$

The mean value of  $\mu$ , averaged over a canonical ensemble might be expressed [15] by Euler gamma function  $\Gamma(x)$  and the incomplete gamma function  $\gamma(x, z)$  [16],

$$\langle \mu \rangle = \frac{1}{(\nu/2)^2} \frac{\gamma(2 + \nu/2, \nu N/2)}{\Gamma(\nu/2)}. \tag{3.9}$$

The parameter  $\nu$  is equal to 1 for orthogonal, 2 for unitary and 4 for symplectic ensemble. The above formula might be simplified for particular values of  $\nu$ , but in the limit of large  $N$  one obtains a simple general result  $\langle \mu \rangle \approx (\nu + 2)/\nu$ . Figure 3 shows the number of relevant states  $M := N/\langle \mu \rangle$  as a function of the matrix size  $N$ . Data obtained for matrices typical to CUE follow the curve given by (3.9) with  $\nu = 2$ , which for large  $N$  tends to a straight line with the slope  $\frac{1}{2}$ .

As a complementary measure of localization one may use the Shannon entropy  $H_l$  of the eigenvector  $|\varphi_l\rangle$  [17]:

$$H_l := - \sum_{k=1}^N y_{lk} \ln(y_{lk}). \tag{3.10}$$

Mean entropy of eigenvectors averaged over Dyson ensembles of unitary matrices can be found analytically [18] and expressed by means of the digamma function  $\Psi(x)$  [16],

$$\langle H_S \rangle = \Psi\left(\frac{\nu N}{2} + 1\right) - \Psi\left(\frac{\nu}{2} + 1\right) \tag{3.11}$$

with  $\nu = 1$  and 2 for COE and CUE, respectively. Numerical results of the mean entropy of eigenvectors of 600 matrices typical of CUE is shown in figure 4 as a function of the matrix

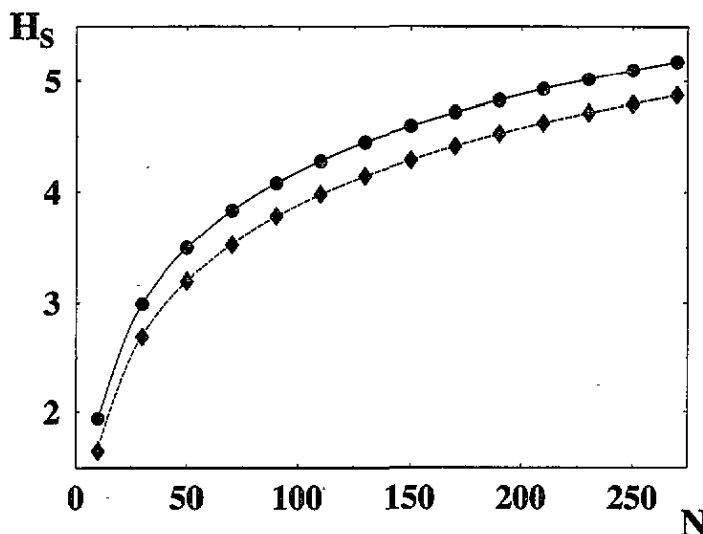


Figure 4. Dependence of entropy of eigenvectors  $H_S$  on the matrix size  $N$  for CUE ( $\circ$ ) and COE ( $\diamond$ ). Smooth curves represent (3.11) with  $\nu = 2$  (full curve) and  $\nu = 1$  (dashed curve).

size  $N$ . Note excellent agreement of the numerical data ( $\diamond$ ) with the full curve representing (3.11) with  $\nu = 2$ .

The entire information about statistical properties of eigenvectors is contained in the distribution of eigenvector components  $P(y)$ . It is known [6, 19, 20] that for Gaussian or circular ensembles eigenvector statistics tends in the limit of large  $N$  to the  $\chi^2_\nu$  distribution

$$P_\nu(y) = \frac{(\nu/2)^{(\nu/2)}}{\Gamma(\nu/2)} \left(\frac{y}{\langle y \rangle}\right)^{\nu/2-1} \exp\left[-\frac{\nu y}{2\langle y \rangle}\right] \tag{3.12}$$

where the number of degrees of freedom  $\nu$  equals 1 for the orthogonal and 2 for the unitary ensemble. Since this distribution peaks around zero, it is convenient to use a logarithmic scale and to study  $P[\log(y)]$ . Figure 5 shows the eigenvector distribution of CUE matrices with the mean value  $\langle y \rangle$  normalized to unity. Observe good agreement with the distribution (3.12) (with  $\nu = 2$ ) represented in the figure by a full curve.

It is worth adding that the above formula with  $\nu = 2$  also describes the distribution of squared elements of the CUE matrices. We checked that the CUE matrices constructed in the way described above possess this property and obtained for the distribution of elements a histogram similar to that shown in figure 5.

#### 4. Numerical generation of matrices typical for COE

In principle it is possible to generate in an analogous manner matrices from the COE by an appropriate restriction of the number and ranges of the Euler angles. In practice, however, we found it more effective to use another method [21]. First observe that, as already pointed out (cf (2.6)), a symmetric unitary matrix can be written as a product of a unitary matrix and its transpose. From (2.6) we have

$$dS = U^T dU + dU^T U. \tag{4.1}$$



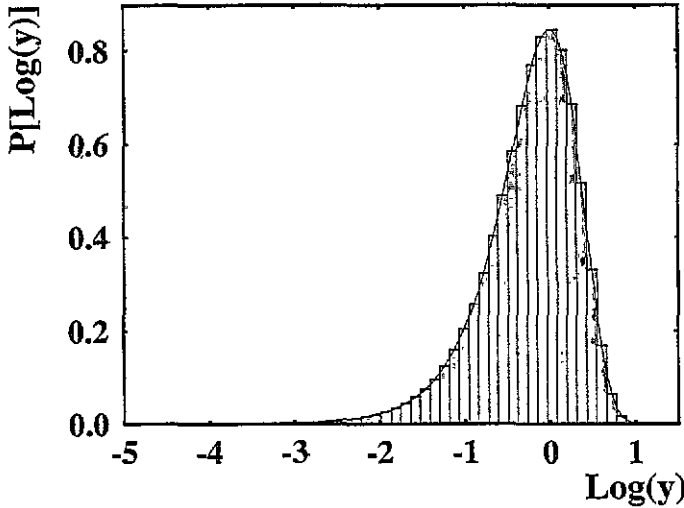


Figure 5. Eigenvector statistics  $P[\log(y)]$  for 600 CUE matrices and the corresponding  $\chi^2_{\nu=2}$  distribution.

From the unitarity of  $U$  we have immediately  $dU^T = -U^T dU^* U^T$ , where  $*$  denotes the complex conjugation. Hence

$$dS = U^T(dUU^\dagger - dU^* U^T)U. \tag{4.2}$$

According to (2.1)  $dU = idXU$ , where we put  $W = 1, V = U$ . Hence from (4.2)

$$dS = U^T(idX + idX^*)U = U^T(2i dX^1)U \tag{4.3}$$

which, upon comparison with (2.7) gives

$$dY = 2 dX^1. \tag{4.4}$$

It is now clear from (2.2) and (2.8) that drawing  $S = U^T U$  from COE is equivalent (after a trivial rescaling) to drawing  $U$  from CUE. Moreover, if  $\{U_i, i = 1, 2, \dots\}$  is a CUE sequence, then the sequence  $\{U_i^T U_i, i = 1, 2, \dots\}$  has the properties of the COE sequence.

We constructed matrices  $U$  typical to CUE as described in the previous section and obtained symmetric matrices  $S = U^T U$ . Superimposing data taken of 1000 unitary matrices of size  $N = 100$  we collected  $10^5$  spacings to the histogram  $P(s)$ . This amount of data is sufficient [22] to distinguish between the Wigner surmise

$$P_W(s) = \frac{\pi}{2} s e^{-4s^2/\pi} \tag{4.5}$$

obtained for  $2 \times 2$  matrices and the exact GOE formula derived by Mehta and Des Cloizeaux [23] (valid also for COE). Figure 6 shows the level statistics for COE matrices. The  $\chi^2$  test gives for Wigner surmise (dashed curve) a confidence level less than  $10^{-6}$ , while the numerical data fit to the COE formula (full curve) with an acceptable confidence-level equal to 0.2. In order to make the distinction between both distributions easier we plot in figure 7 the same data in a magnified scale with respect to the Wigner surmise (horizontal line) and represent the COE distribution by a full curve. The difference between the numerical results and the Wigner surmise is thus evident. Since the original formula of Mehta and Des Cloizeaux written as an infinite product is not handy to use, we apply a power expansion, derived by Dietz and Haake [24].

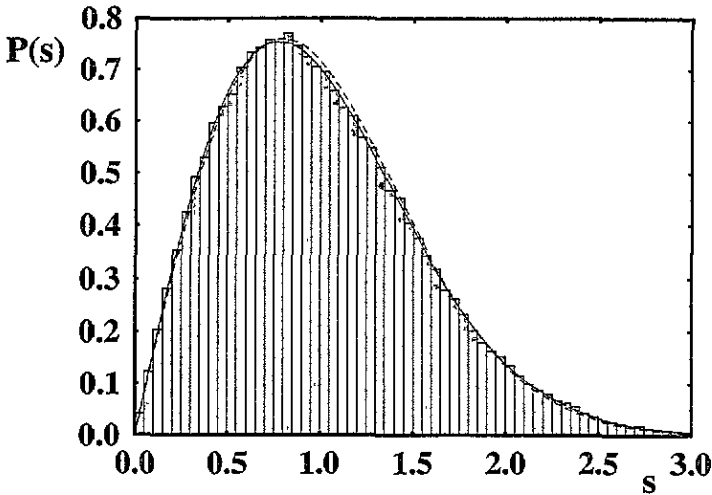


Figure 6. Level spacing distribution  $P(s)$  for  $10^5$  data collected from 1000 matrices of size  $N = 100$ . The full curve denotes exact COE (GOE) distribution and dashed curve is the Wigner surmise.

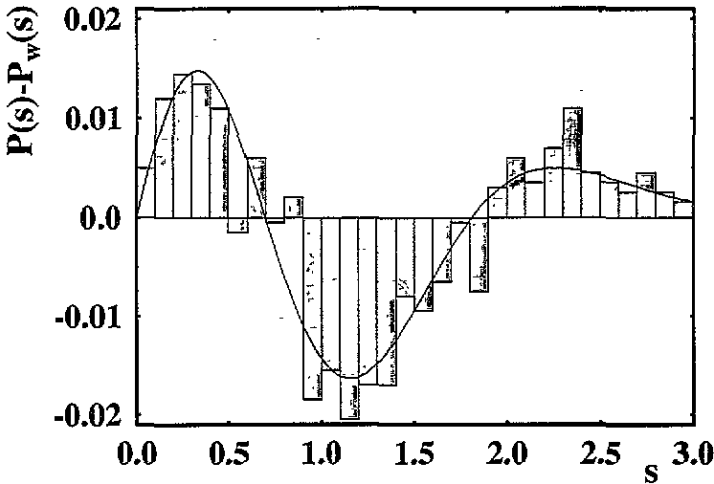


Figure 7. COE level-spacing distribution measured with respect to the Wigner surmise  $P_W(s)$ .

Long-range correlations of spectra of matrices typical to COE comply to predictions of random matrices. Numerical data of the number variance  $\Sigma^2(L)$  are represented by diamonds in figure 2, while the dashed curve denotes the approximate ( $L > 1$ ) COE formula [7, 2]

$$\Sigma^2_o(L) = \frac{2}{\pi^2} \left( \ln(2\pi L) + 1 + \gamma - \frac{\pi^2}{8} \right). \tag{4.6}$$

Eigenvectors of the matrices  $U^T U$  possess all properties typical to COE. As it is shown in figure 3, the number of relevant states for COE tends, for large matrices, to  $N/3$ . The

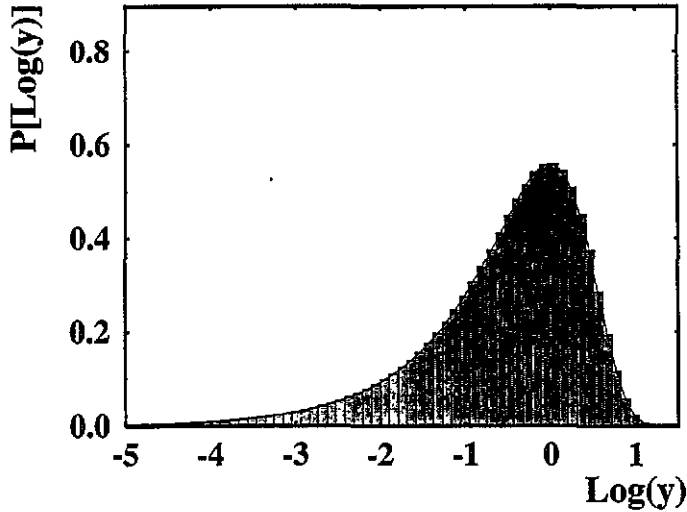


Figure 8. Eigenvector statistics  $P[\log(y)]$  for 1000 COE matrices and the corresponding  $\chi^2_{\nu=1}$  distribution.

mean entropy of COE eigenvectors, represented in figure 4 by  $(\diamond)$ , confers to (3.11) with  $\nu = 1$ . Eigenvector statistics of COE matrices is displayed in figure 8. Numerical results are well described by the  $\chi^2_{\nu}$  distribution (3.12) with  $\nu = 1$ .

## 5. Concluding remarks

In the preceding sections we have shown how to generate random matrices typical to unitary and orthogonal circular ensembles. Matrices generated according to the distribution (3.5) are typical to CUE with respect to the level-spacing distribution, number variance, entropy of eigenvectors, participation ratio and eigenvector statistics. Matrices typical to COE are generated as products of matrices from CUE and their transposes.

As already mentioned, ensembles of random matrices were used to describe various properties of quantum systems exhibiting chaos. Recently a considerable interest was aroused by investigations of transitions between different universality classes when parameters of the system change. Such a situation happens when a (generalized) time-reversal symmetry of a quantum system is broken and corresponds to a transition from orthogonal to unitary ensemble of random matrices. Such a transition was investigated in the case of the kicked rotator [25] and the kicked top [26]. In the latter work it was found that in some aspects the situation differs from the analogous one involving Hermitian matrices [27]. It is thus interesting to find whether these differences are only characteristic to the particular system investigated in [26] or are rather typical for unitary matrices. Using our methods of generating random unitary ensembles we hope to answer this question in the forthcoming publication.

## Acknowledgments

We are grateful to Barbara Dietz for providing a computer routine, which gives the GOE level-spacing distribution. It is a pleasure to thank J Gancarzewicz and J Zakrzewski for

helpful remarks. This work was supported by Polish KBN Grant number 2-P302-035-05.

## References

- [1] Dyson F J 1962 *J. Math. Phys.* **3** 140
- [2] Bohigas O 1991 *Chaos and Quantum Physics Les Houches Session LII 1989* ed M J Giannoni and A Voros (Amsterdam: North-Holland)
- [3] Haake F 1991 *Quantum Signatures of Chaos* (Springer: Berlin)
- [4] Dyson F J and Mehta M L 1963 *J. Math. Phys.* **4** 701
- [5] Mehta M L 1990 *Random Matrices* 2nd edn (New York: Academic)
- [6] Porter C E 1965 *Statistical Theories of Spectra: Fluctuations* ed C E Porter (New York: Academic)
- [7] Brody T A, Flores J, French J B, Mello P A, Pandey A and Wong S S M 1981 *Rev. Mod. Phys.* **53** 385
- [8] Blümel R and Smilansky U 1990 *Phys. Rev. Lett.* **64** 241
- [9] Blümel R, Dietz B, Jung C and Smilansky U 1992 *J. Phys. A: Math. Gen.* **25** 1483
- [10] Csordás A and Šeba P 1994 *Chaos* **3** in press
- [11] Hua L K 1963 *Harmonic Analysis of Functions of Several Variables in the Classical Domains* (Providence, RI: American Mathematical Society)
- [12] Hurwitz A 1887 *Nachr. Ges. Wiss. Gött. Math.-Phys. Kl.* **71**
- [13] Girko V L 1990 *Theory of Random Determinants* (Dordrecht: Kluwer)
- [14] Weaire D and Williams A R 1977 *J. Phys. C: Solid State Phys.* **10** 1239
- [15] Życzkowski K 1990 *J. Phys. A: Math. Gen.* **23** 4427
- [16] Spanier J and Oldham K B 1987 *An Atlas of Functions* (Washington: Hemisphere)
- [17] Casati G, Molinari L and Izrailev F 1990 *Phys. Rev. Lett.* **64** 1851
- [18] Jones K R W 1990 *J. Phys. A: Math. Gen.* **23** L1247
- [19] Kuś M, Mostowski J and Haake F 1988 *J. Phys. A: Math. Gen.* **21** L1037
- [20] Haake F and Życzkowski K 1990 *Phys. Rev. A* **42** 1013
- [21] Życzkowski K 1993 *Acta Phys. Pol. B* **24** 967
- [22] Dietz B and Życzkowski K 1991 *Z. Phys. B* **84** 157
- [23] Mehta M L and Des Cloizeaux J 1971 *Indian J. Math.* **3** 329
- [24] Dietz B and Haake F 1989 *Europhys. Lett.* **9** 9
- [25] Blümel R and Smilansky U 1992 *Phys. Rev. Lett.* **69** 217
- [26] Lenz G and Życzkowski K 1992 *J. Phys. A: Math. Gen.* **25** 5539
- [27] French J B, Kota V K B, Pandey A and Tomsovic S 1988 *Ann. Phys., NY* **181** 198